

Interannual variations in precipitation: The effect of the North Atlantic and Southern oscillations as seen in a satellite precipitation data set and in models

Elizabeth A. Kyte,^{1,2} Graham D. Quartly,¹ Meric A. Srokosz,¹ and Michael N. Tsimplis¹

Received 30 January 2006; revised 16 May 2006; accepted 17 July 2006; published 29 December 2006.

[1] Precipitation is a parameter that varies on many different spatial and temporal scales. Here we look at interannual variations associated with the North Atlantic Oscillation (NAO) and the Southern Oscillation (SO), comparing the spatial and temporal changes as shown by three data sets. The Global Precipitation Climatology Project (GPCP) product is based upon satellite data, whereas both the National Centers for Environmental Prediction (NCEP) and European Centre for Medium-Range Weather Forecasts (ECMWF) climatologies are produced through reanalysis of atmospheric circulation models. All three products show a consistent response to the NAO in the North Atlantic region, with negative states of the NAO corresponding to increases in precipitation over Greenland and southern Europe, but to a decrease over northern Europe. None of the climatologies display any net change in total rainfall as a result of the NAO, but rather a redistribution of precipitation patterns. However, this redistribution of rain is important because of its potential effect on oceanic overturning circulation. Similarly, all three data sets concur that the SO has a major effect on precipitation in certain tropical regions; however, there is some disagreement amongst the data sets as to the regional sensitivity, with NCEP showing a much weaker response than GPCP and ECMWF over Indonesia. The GPCP and NCEP climatologies show that the various phases of El Niño and La Niña act to redistribute, rather than enhance, the freshwater cycle. Given that the models incorporate no actual observations of rain, and are known to be imperfect, it is surprising how well they represent these interannual phenomena.

Citation: Kyte, E. A., G. D. Quartly, M. A. Srokosz, and M. N. Tsimplis (2006), Interannual variations in precipitation: The effect of the North Atlantic and Southern oscillations as seen in a satellite precipitation data set and in models, *J. Geophys. Res.*, *111*, D24113, doi:10.1029/2006JD007138.

1. Introduction

[2] Varying rainfall patterns are an important component of climate change, with variations in intensity and location of the main rain systems being both a response to atmospheric change, and potentially, influencing climate change through modification of the overturning ocean circulation (the so-called “conveyor belt”) and also by affecting ice sheet growth or decay. Both the ocean and atmosphere significantly influence precipitation variability on a number of spatial and temporal scales, and may also act together to drive climate change to an almost global extent [Petterssen, 1969; Khalil *et al.*, 1992]. Whilst there are long and detailed records of rainfall over land in many of the developed regions of the world, accurate surface measurements at sea are scarce, since the measurement of precipitation over the oceans is a particularly challenging task. Accurate measure-

ments of oceanic precipitation are essential in order to quantify precipitation variability on both regional and global scales. Also, precipitation at sea is an important aspect of the forcing of oceanographic models; inaccurate representation of the precipitation variations associated with El Niño, for example, may prevent a model from getting the oceanographic response correct. Traditional methods of precipitation measurement rely on in situ measurement techniques, utilising ships or buoys to collect precipitation data. However, the very nature of precipitation itself (occurring on limited and variable time and space scales) renders these techniques inaccurate, biased and often unreliable [Barrett and Martin, 1981; Quartly *et al.*, 2002]. Tucker [1961] developed a method of quantifying oceanic rainfall on the basis of ships’ reports of “Present Weather”. However, the concentration of traffic along well-defined shipping routes leaves many regions poorly sampled, and evaluation of such records for the well-sampled North Atlantic suggests errors in the mean rainfall of around 50% [Dorman and Bourke, 1981].

[3] It is for this reason that researchers have turned to oceanic precipitation records based on satellite data, and output from numerical weather forecast models. A companion

¹National Oceanography Centre, Southampton, UK.

²Now at School of Ocean Sciences, University of Wales, Bangor, Anglesey, UK.

paper (G. D. Quartly et al., An intercomparison of global oceanic precipitation observations, submitted to *Journal of Geophysical Research*, 2006; hereinafter referred to as Quartly et al., submitted manuscript, 2006) discusses the changes in the availability of source data used to form these products, and compares how four such climatologies portrayed the mean global precipitation field and its seasonal variation. This paper examines how three of those data sets represent longer-term interannual variations associated with two of the most pronounced regional cycles, the North Atlantic Oscillation (NAO) and the Southern Oscillation (SO). By applying identical analysis techniques to these three independent data sets over a common period, we can more usefully compare results between them, giving greater confidence to results common to all, and also assessing how well standard weather forecast models can portray such interannual phenomena.

[4] The NAO is the dominant atmospheric mode by which winter climate varies in the North Atlantic region, (M. Visbeck, North Atlantic Oscillation, <http://www.ideo.columbia.edu/res/pi/NAO>, 11 May 2004; hereinafter referred to as Visbeck, 2004). It is a measure of the temporal fluctuations in zonal wind stress across the North Atlantic Ocean caused by changes in the atmospheric pressure gradient between the subtropical cyclone belt and the subpolar low, near Iceland. The NAO index is a quantitative measure of these changes, derived through analysis of normalized mean winter pressure anomalies at the Azores and Iceland [Bromwich et al., 1999]. The NAO index may take a positive or negative value, where positive indices indicate a stronger than usual subtropical high-pressure center and a deeper than normal Icelandic low. This leads to warm wet winters in Europe, and cold dry winters in northern Canada and Greenland. A negative NAO index indicates the presence of a weak subtropical high and a weak Icelandic low. This results in fewer storms crossing the North Atlantic, with northern European temperatures dropping. Moist air is brought into the Mediterranean during an NAO negative phase. Farther north, Greenland experiences milder winter temperatures (Visbeck, 2004). Studies have shown that there is a strong correlation between the NAO index and precipitation in northwest Africa, Azores, Portugal and Spain [Goodess and Jones, 2002], whilst long-term dry winters experienced for the past decade over southern Europe and the Mediterranean can be linked to a recent long-term positive NAO phase [Hurrell, 1995; Tsimplis and Josey, 2001]. In most cases, the effects of NAO are only clear during winter, defined, in this context, as December to March inclusive.

[5] El Niño-Southern Oscillation (ENSO) is a coupled ocean-atmosphere phenomenon occurring principally within the tropical Pacific Ocean, but having ramifications further afield through atmospheric teleconnections. The normal atmospheric circulation involves easterly trade winds converging along the intertropical convergence zone (ITCZ) just north of the equator, uplift occurring at the western edge of the Pacific, with the zonal Walker cells being completed by subsidence over the eastern Pacific and western Indian Ocean. Under these conditions the surface waters form a “warm pool” at the western edge of the equatorial Pacific, and the majority of the precipitation falls over this warm pool, along the ITCZ, and in a band running southeast from

Papua New Guinea termed the South Pacific convergence zone (SPCZ).

[6] An El Niño event occurs when the trade winds are weaker, with associated changes in sea surface temperature and the ascending branch of the Walker circulation moving toward the central Pacific, leading to an eastward migration of the areas of rainfall. Changes have been observed in frontal systems, monsoonal cycles and tropical cyclones, resulting in both flooding and drought events on a number of spatial and temporal scales (see Quartly et al. [2000], Georgakakos [1998], Barlow et al. [2002], and Nicholson et al. [2001] for examples of precipitation variability with El Niño events). The complementary phase of the atmospheric circulation, La Niña, is characterized by enhanced trade winds, with the region of uplift of moist air being translated further west over Indonesia and parts of the Indian Ocean. El Niño and La Niña are two facets of an irregular oscillation, occurring every 3–7 years.

[7] This study quantifies the relationship between changes in atmospheric pressure differences and precipitation on both regional and global scales. In doing so we exploit a variety of data resources, showing where there is a consensus on the changing patterns of precipitation, but also highlighting where there is disagreement between the data sets. There is no single “correct” data set, especially over the ocean; however, contrasting the NAO- and SO-related patterns in these relatively long time series can help pinpoint possible deficiencies in each one, as well as establish consistent features. The next section of this paper outlines the precipitation data sets used within this study — data from satellite remote sensing, and output from numerical weather forecast models. Sections 3 and 4 then demonstrate the rôle that both the NAO and the SO play in the interannual variability of precipitation, as portrayed within these data sets. Our conclusions appear in the last section of this paper.

2. Precipitation Data Sets

[8] Three different precipitation data sets were obtained, and monthly maps generated on a global $2.5^\circ \times 2.5^\circ$ grid. A brief synopsis of each data set is provided below. Although the two data sets based on numerical weather forecast output extend back more than 40 years, the analysis of all three data sets was confined to the 22-year period in common (between January 1979 and December 2000). All three data sets suffer from some changes in their characteristics as new sources of information become available and are incorporated (Quartly et al., submitted manuscript, 2006). However, use of a much shorter period would not encompass sufficient El Niño events and range of NAO values for general conclusions to be drawn.

2.1. Global Precipitation Climatology Project (GPCP)

[9] The GPCP version 2 combined satellite gauge data set was developed by the NASA/Goddard Space Flight Center’s Laboratory for Atmospheres. This product integrates a number of different satellite data sets, plus rain gauges over land. The period of interest (1979–2000) can be divided into three phases according to the primary satellite data sets that were available. Prior to 1986 the only satellite data used were based on cloud top temperatures from low Earth orbit

infrared sensors; after this period, geostationary satellites were available, giving more frequent coverage of the band 40°S to 40°N. The other major change corresponds to the addition of microwave data from SSM/I and TOVS from July 1987 onward (excluding December 1987). The use of microwave precipitation sensors provides better regionally varying calibration for the infrared sensors, which only respond to cloud cover. Note that there is no incorporation of TRMM data in this product, so no change is expected at the start of December 1997. The reader is directed to *Adler et al.* [2003] for further details of the GPCP product.

2.2. National Centers for Environmental Prediction (NCEP)

[10] The U.S. NCEP and National Center for Atmospheric Research (NCAR) performed a reanalysis of much of the meteorological data from 1949 to present, using data assimilation within the NCEP global spectral model. The NCEP data set combines information from a number of different sensors, including upper air sonde observations of temperature, humidity and wind; aircraft-based observations of wind and temperature; land and oceanic reports of surface pressure and temperature and wind profile data from a satellite-based vertical sounder [*Kistler et al.*, 2001]. No actual precipitation data are used, as these are difficult to assimilate into models. Although reprocessing was done throughout with the same model, the entire record is not consistent. For example, the period 1949–1957 is considered less reliable than later years because of fewer upper air observations being made during this time. However, there are only minimal changes in the input data during the period of interest within this study (1979–2000) (see *Kistler et al.* [2001] for further details).

2.3. European Centre for Medium-Range Weather Forecasts (ECMWF)

[11] The European Centre for Medium-Range Weather Forecasts (ECMWF) has also performed a reanalysis of meteorological data spanning the period 1957 to 2002. Their reanalysis used many sources of data in common with NCEP, but also included other input such as wind speed from scatterometers and data from previous large-scale atmospheric circulation projects, such as GATE, FGGE and TOGA-COARE [*Uppala et al.*, 2004]. However, there are known problems associated with the humidity assimilation [*Hagemann et al.*, 2005], which result in an overestimation of precipitation in the tropics. *Troccoli and Källberg* [2004] suggest adjusting the forecast output between 30°S and 30°N to bring them into line with other estimates (such as GPCP). As we wish to preserve the independence of our three data sets in order to contrast their representations of interannual phenomena, no such adjustments were applied here. However, any observed inconsistencies within this data set (particularly within the tropics) must therefore be evaluated in the light of this known problem.

[12] In order to highlight the effect upon interannual variations of the NAO and ENSO, precipitation anomalies were calculated by subtracting the mean map of January precipitation from each individual January and so on. Thus

by definition, the mean anomaly for each $2.5^\circ \times 2.5^\circ$ pixel is zero.

3. Winter Precipitation and the NAO

[13] It is the wintertime NAO that exerts a particularly strong influence on regional climate in the North Atlantic [*Ogi et al.*, 2003] (see also T. Osborn, North Atlantic Oscillation, http://www.cru.uea.ac.uk/~timo/projpages/nao_update.htm, 25 June 2004). Consequently, all analysis performed within this paper uses only an index averaged over December to March (hereafter DJFM NAO), based on the monthly NAO values provided by the Climatic Research Unit (CRU, North Atlantic Oscillation, <http://www.cru.uea.ac.uk/cru/data/nao.htm>, 20 June 2004).

[14] To examine the change of precipitation with NAO in these three data sets, we calculated a map of mean precipitation anomalies for each winter (December to March), and for each individual grid point regressed the variations in precipitation against the DJFM NAO index. Figures 1a–1c show the results for the North Atlantic and environs. Values are only plotted if their difference from zero is significant at the 95% confidence level. The three data sets agree in their basic broad patterns. They have regions of positive correlation over northern Europe (implying an increase in rainfall with increased NAO index) and regions of negative correlation over Greenland and southern Europe, with values of sensitivity typically being 10 mm month^{-1} for a unit change in DJFM NAO index. The results for GPCP are slightly different from the others. Firstly, the regions of significant correlation are somewhat smaller. Secondly, the magnitude of the sensitivity is somewhat less for both positive and negative correlation regions.

[15] If the regression analysis is extended to the whole global precipitation field (figure not shown), a few other regions show apparent pockets of sensitivity in two or three of these data sets. Siberia shows a negative correlation with DJFM NAO, which may be due to the Icelandic low also affecting the circulation there, via the so-called Arctic Oscillation. The other affected regions are southeast of Australia and to the west of Chile. However, as we are not aware of any plausible mechanism for such teleconnections we cannot exclude the possibility that these may be statistical artefacts. Nevertheless we observe that such correlations have also been reported elsewhere, for example in relation to NAO influence on extreme sea levels [*Woodworth and Blackman*, 2004].

[16] *Josey and Marsh* [2005] performed a similar regression of NCEP precipitation against NAO index (their Figure 6c), but using a September to March average and also including NCEP output from 1960 to 1978. Although broadly similar results were found, the longer data set gives them larger values for the sensitivity per unit NAO index, though possibly this is an artefact of a slight long-term trend in NCEP records, as the majority of the NAO negative states are in the first half of their analysis period, and the majority of the NAO positives are in the second half. They do not show precipitation over land, but their geographical patterns over the ocean also appear to be displaced further west, such that there is no longer a negative response to NAO over Greenland and the Labrador Sea. *Bojariu and Reverdin* [2002] also restrict themselves to only over-ocean

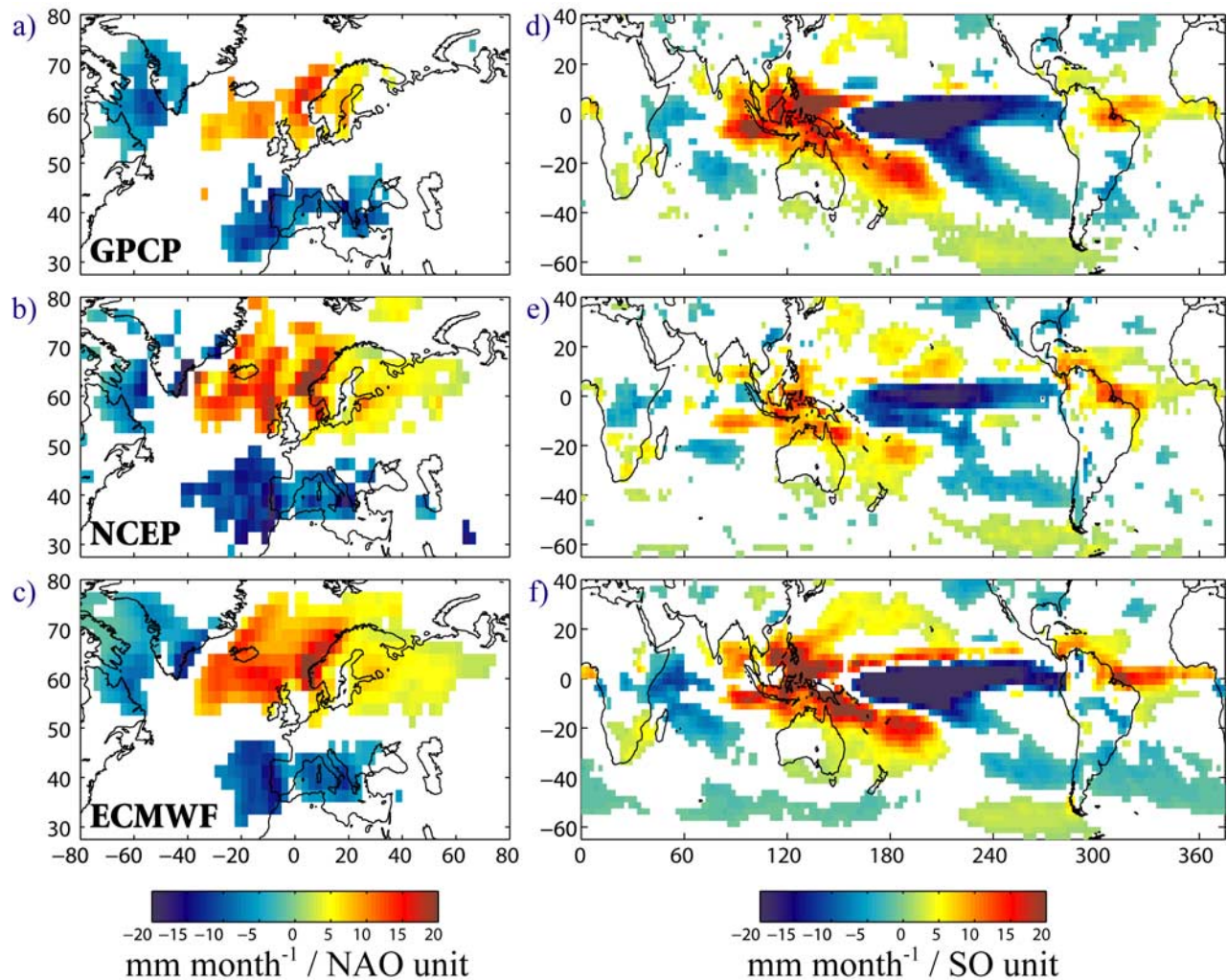


Figure 1. (left) Sensitivity of precipitation to NAO index (mm/month per unit change in the December to March (DJFM) NAO index): (a) Global Precipitation Climatology Project (GPCP), (b) National Centers for Environmental Prediction (NCEP), (c) European Centre for Medium-Range Weather Forecasting (ECMWF). (right) Sensitivity of precipitation to SO index (mm/month per unit change in SOI): (d) GPCP, (e) NCEP, (f) ECMWF.

data; consequently their results based on EOF analysis of a restricted domain, give only a hint of the response over the Labrador Sea.

[17] To make a clearer intercomparison of the magnitudes of the variations within these three data sets, we determine an areal mean precipitation anomaly for three areas representing Greenland, northern Europe, and southern Europe. The areas for averaging within each data set are defined by the regions of significant correlation between precipitation and the NAO, as seen in Figures 1a–1c. For each, the month-to-month variations are of order 10 mm month^{-1} (Figures 2b–2d), with all three data sets yielding very similar variations for Greenland and northern Europe, but with a little less agreement for southern Europe. For comparison, the DJFM NAO index is displayed in Figure 2a.

[18] It has been established that during positive NAO phases that Greenland and southern Europe will experience a reduction in precipitation, whilst the North Atlantic and northern Europe see an increase. However, it is not clear whether these increases and reductions affect the total

precipitation budget. Time series plots of total precipitation anomalies over the North Atlantic and neighbouring land masses are shown in Figure 2e. The GPCP curve shows a step change of $\sim 10 \text{ mm month}^{-1}$ in 1988, the time when SSM/I data start being incorporated; a revision to the GPCP (June 2006) shows no such abrupt change (see Appendix A). The curves for the three data sets appear to show some year-to-year changes in common, but many differ. None of the three data sets shows a clear dependence of the total precipitation upon the NAO index. Thus within the measurement uncertainties of these data sets, the NAO appears to redistribute precipitation patterns around the North Atlantic, Europe and Greenland, but does not cause any net change in precipitation over this larger area.

4. Precipitation and ENSO

[19] There are many indices for charting the progress of an El Niño; here we use the Southern Oscillation Index (SOI), which is defined as the normalized pressure differ-

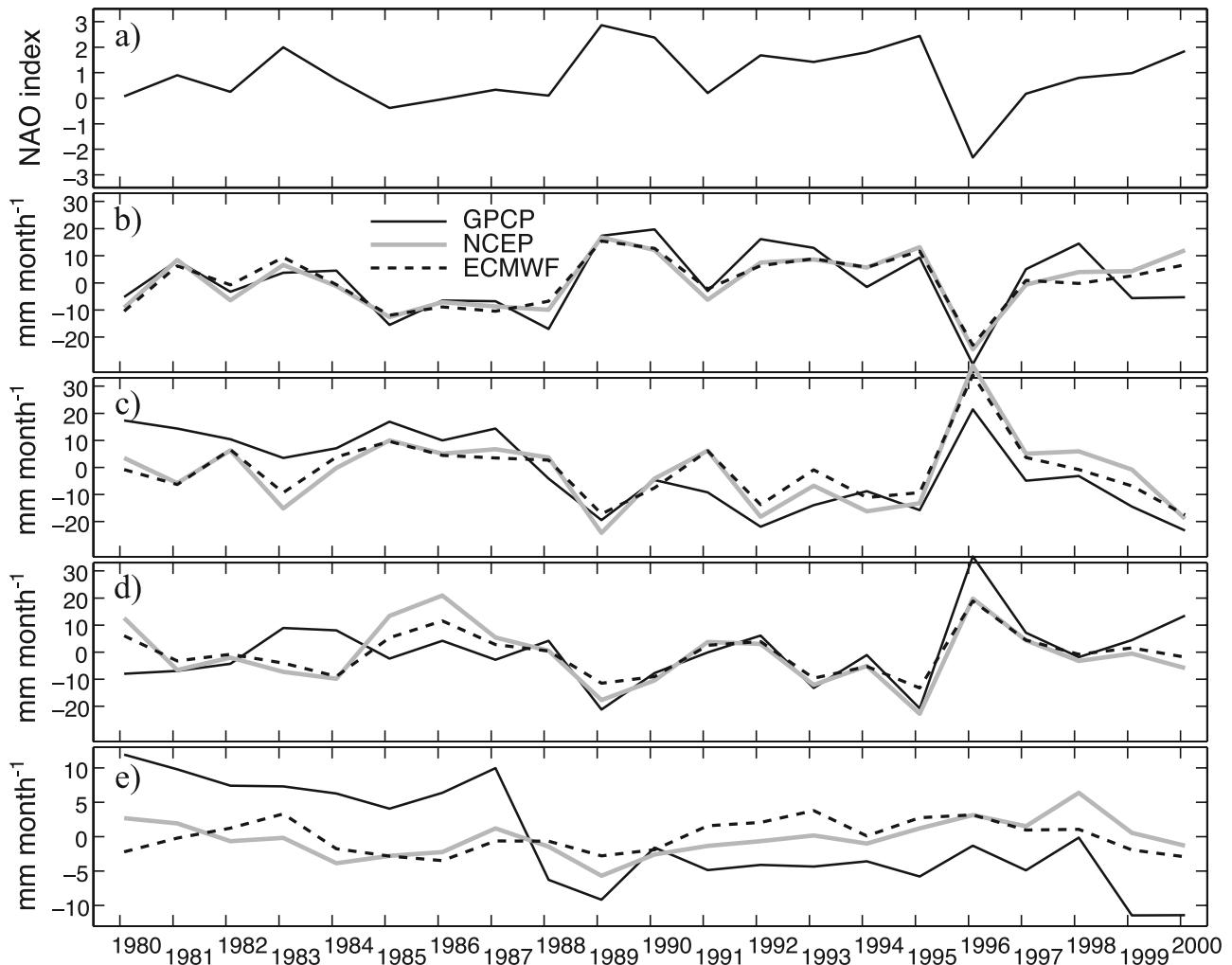


Figure 2. Winter precipitation anomalies in the North Atlantic. (a) NAO index averaged over December to March; average precipitation anomaly over (b) northern Europe region; (c) southern Europe region; (d) Greenland region; and (e) North Atlantic and surrounding land masses (80°W to 60°E , 30° – 80°N). The key for the lines in Figures 2c–2e is as in Figure 2b. Note the scale is different for Figure 2e.

ence between Tahiti and Darwin. This was standardised using the approach outlined by Trenberth [1984]. Within this particular definition of the SOI, large negative values represent El Niño events, with La Niña episodes being characterised by large positive indices. The SOI values used within this study were obtained from the Climate Analysis Section at the Climate and Global Dynamics Division of NCAR (CAS, Southern Oscillation Index based upon annual standardization, <http://www.cgd.ucar.edu/cas/catalog/limind/soiAnnual.html>, 13 August 2004).

4.1. Regression Analysis

[20] Figures 1d–1f show maps of sensitivity to SOI for each data set, where points are only plotted if their difference from zero is significant at the 95% confidence level. Again all these data sets exhibit the same basic patterns. There is a region of strong negative correlation (implying increased rainfall during El Niño) in the central and eastern Pacific. This is because as El Niño develops the warm pool of water migrates eastward across the ocean basin, bringing the northern end of the SPCZ with it, plus a broadening and

intensification of the ITCZ. The ITCZ also moves south by up to 5° resulting in a thin band of positive correlation along the northern edge of its normal position. There are also two important areas of positive correlation in the tropical Atlantic, and over Indonesia, straddling both the western Pacific and eastern Indian oceans. A further zone of positive correlation, running from the eastern Mediterranean to central eastern Africa and to the ocean east of Madagascar, is consistent within all three data sets. Note that this is not a full representation of the precipitation changes in an El Niño cycle, as some regions experience a lagged effect not coinciding with either the peaks of the El Niño or La Niña phases. For example, Nicholson [1997] concluded that a reduction in African rainfall occurs several months after the peak of ENSO in response to increased surface temperatures in the Atlantic and Indian oceans.

[21] Further analysis of Figures 1d–1f shows that the precipitation changes due to the Southern Oscillation are weaker in NCEP than the other two data sets. A considerably weaker and smaller region of sensitivity is noted over Indonesia, with reduced movement of the SPCZ also being

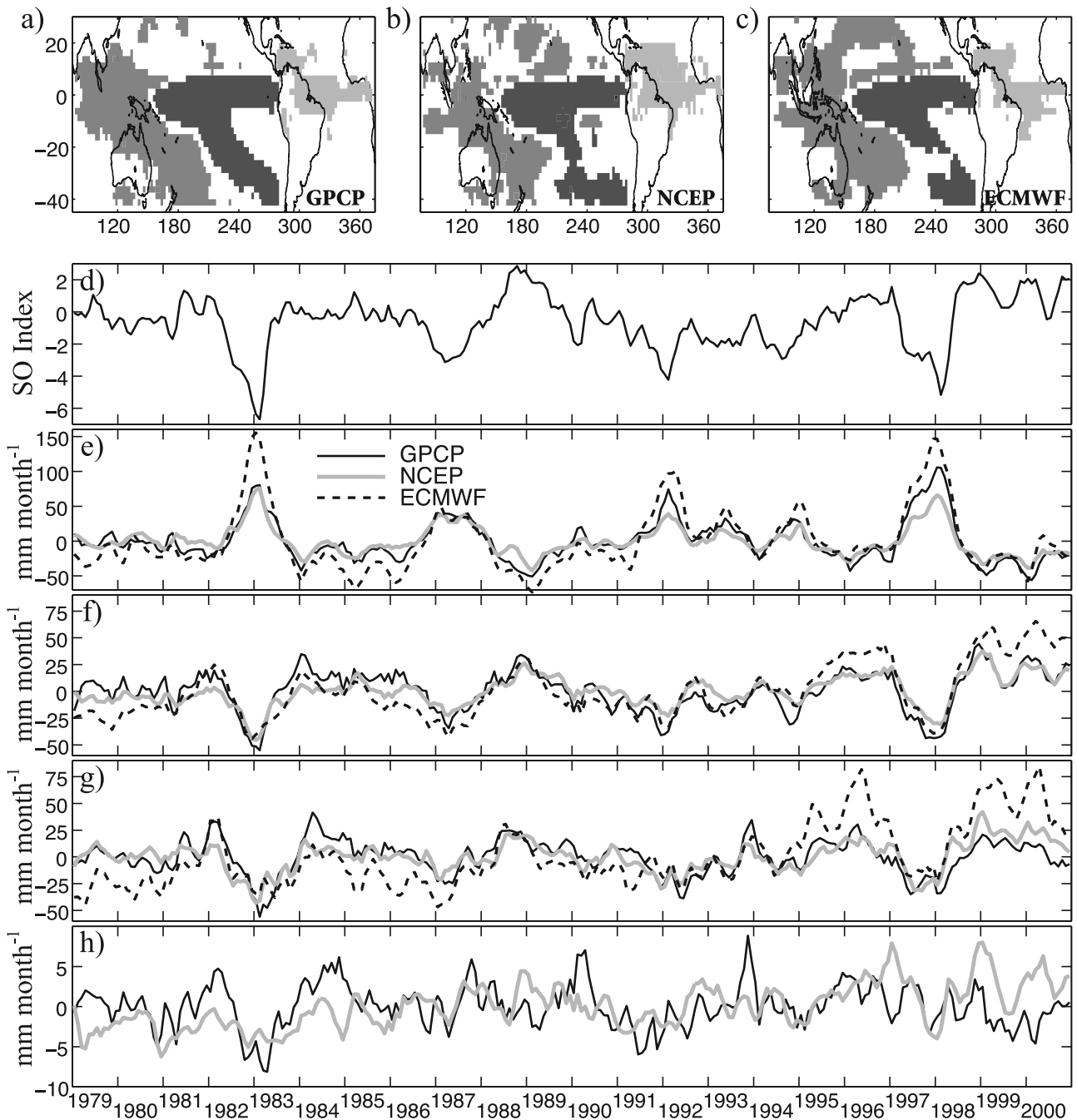


Figure 3. Interannual precipitation anomalies in the tropical Pacific and environs. Top row shows regions of sensitivity over which anomalies were averaged for (a) GPCP, (b) NCEP, and (c) ECMWF. Time series plots are of (d) Southern Oscillation Index, (e) precipitation anomaly for eastern Pacific, (f) western Pacific and east of Australia, and (g) tropical Atlantic. (h) GPCP and NCEP anomalies averaged over entire tropical region illustrated. Figures 3d–3h have had a 3-month running mean applied to allow the seasonal to interannual scales to be easily seen. The key for the lines in Figures 3f–3h is as in Figure 3e.

apparent. This is consistent with the wind field in NCEP that is weaker in magnitude and convergence than other wind climatologies [Josey et al., 2002]. It should be noted that even during years that are neither El Niño or La Niña, the mean position and orientation of the SPCZ in models is

rather different to that shown by satellite data [Trenberth and Guillemot, 1998; Taylor, 2000].

[22] We calculate monthly precipitation anomalies averaged over each of the three main regions of sensitivity. The definitions of the regions used were different for each of the data sets (see Figures 3a–3c) because they showed different

locations for positive and negative correlation. The resultant monthly regional anomalies have then had a 3-month running mean applied to make comparisons easier (Figures 3e–3h). All the data sets show an increase in eastern Pacific precipitation associated with each of the four main El Niño events of this period, viz. 1982/1983, 1986/1987, 1991/1992 and 1997/1998; they also all show corresponding decreases in the western Pacific. There are also decreases in the tropical Atlantic associated with all four El Niño events, with only the strong 1982/1983 and 1997/1998 ones being particularly pronounced. *Uvo et al.* [1998] note that during El Niño, there is a tendency for positive sea surface temperature anomalies to develop in the Atlantic just north of the equator, with the change in meridional temperature gradient leading to droughts over northern Brazil [*Hastenrath*, 1978]. La Niña may be expected to have the opposite effect to El Niño, but only the 1988/1989 and 1998/1999 events coincide with increases in the western Pacific region (and then not for NCEP).

[23] Figure 3h shows the net sensitivity to SOI over an expanded tropical region (75°–375°E, 40°S to 25°N), as shown in the GPCP and NCEP data sets. The GPCP data set shows an overall decrease for the 1982/1983 El Niño, but not the 1997/1998 one, whereas the reverse is the case for NCEP, with neither showing a clear response to the 1986/1987 event. (The curve for ECMWF is not shown, because it is dominated by a long-term trend, requiring an ordinate range three times that shown.) Given the measurement uncertainties within these data sets plus the different responses to the four major El Niño events of those 22 years, it appears that El Niño acts to redistribute the precipitation within a large “tropical” region, rather than to enhance or diminish the freshwater cycle. The ECMWF data set shows a long-term increase in precipitation, with a marked change in 1991. There are also short-term increases coinciding with the 1982/1983 and 1991/1992 El Niños but not the 1986/1987 and 1997/1998 ones. It has been conjectured that aerosols released by the eruptions of El Chichón (1983) and Pinatubo (1991) may affect the hydrological cycle in the northern tropics and thus partially confound our analysis for ENSO signals. However, in a study taking account of ENSO, *Mass and Portman* [1989] find no clear effect of volcanoes on the precipitation record. However, these apparent inconsistencies between the ECMWF data set and both the NCEP and GPCP products are most likely due to errors within the ECMWF climatology, rather than any observed fluctuations or variability. The ECMWF data set has a known problem related to its humidity assimilation scheme [*Troccoli and Källberg*, 2004] such that the mean estimated precipitation rate in the tropics is ~50% larger than in the other data sets (see *Quartly et al.*, submitted manuscript, 2006, Figure 8j. It seems likely that, for El Niño episodes, the precipitation excess in the eastern Pacific is similarly exaggerated (Figure 3e) leading to net changes when summed over the larger tropical region.

4.2. Comparison With Earlier Work

[24] Many researchers have looked at the effects of ENSO using a single precipitation data set, based either on satellite data, model output or land station records. The common theme of the movement and intensification of the ITCZ and SPCZ has been shown before using GPCP

[*Huffman et al.*, 1997; *Adler et al.*, 2003; *Sohn et al.*, 2004]. An alternative multisatellite climatology, CMAP, gives a similar quantitative change to GPCP for the 1997/1998 El Niño [*Xie and Arkin*, 1997; *Gruber et al.*, 2000]. *Adler et al.* [2001] found ECMWF and GPCP to give similar responses to the 1991/1992 El Niño. Also, a recent numerical model has been shown to give a similar response to GPCP in terms of sensitivity to El Niño [*GFDL*, 2004, Figure 13]. Using an altimeter-derived rainfall climatology, *Quartly et al.* [2000] showed that the spatial changes during the 1997/1998 El Niño were also accompanied by an increased frequency and intensity of rain, leading to a net increase in tropical Pacific rainfall during the event. However, they did not consider the precipitation over land. *Adler et al.* [2003] examined the GPCP data on a global basis, and noted that there were reductions in precipitation over land coinciding with the four main El Niños of the period, but that the total rainfall over both land and sea showed no clear response to the four events. *Dai and Wigley* [2000] note a similar result using CMAP data. Our results concur when a large enough areal average is considered (Figure 3h).

[25] There is a difference in the response of the three data sets near Sumatra: GPCP shows a reduction in rainfall there during ENSO (as for the rest of Indonesia), ECMWF indicates negligible response, and NCEP shows an enhancement in rainfall. Using land station records, *Chang et al.* [2004] had identified this area as having an unusual response: during La Niña the winds converge over Indonesia, with uplift and enhanced rainfall, except for the area between Sumatra and west Borneo as the steep topography reduces the effect of the winds. On the other side of the Indian Ocean, our analysis noted increased precipitation off the eastern coast of Africa correlated with El Niño in all three data sets; this demonstrates a coherent region of increased rainfall that had only been hinted at by the isolated island stations analysed by *Ropelewski and Halpert* [1987], though *Ntale and Gan* [2004] had noted that Tanzania had pronounced rains associated with El Niño. *Nicholson et al.* [2001] showed El Niño to be associated with acute drought in Botswana, possibly via the SO affecting sea surface temperatures in the neighbouring oceans; *Ropelewski and Halpert* [1987] infer that the drought covers a large part of southern Africa. The three data sets we analysed show similar sensitivity here.

[26] Figures 1d–1f also show an area of increased rainfall during El Niño on the east of the North Pacific, and just affecting the Californian coast. The response in this region has been well documented by *Castello and Shelton* [2004], but *Andrews et al.* [2004] note that the magnitude of a specific El Niño event has little bearing on the magnitude of the associated flood event. Floods related to El Niño have also been recorded in Mexico, but significant changes in precipitation are not found there in our analysis. Moving farther south, our three data sets all show a significant reduction in rain in the Caribbean, the tropical Atlantic and over north Brazil, with an increase in south Brazil, Uruguay and Argentina (although the latter response is muted for NCEP). This difference in response between north and south Brazil is attested by land station observations [*Grimm*, 2003]. *Grimm* [2003] states that this effect occurs through the modulation of processes that produce the normal seasonal peak in precipitation during austral summer; and also

comments that in some regions the El Niño response changes sign midway through that season. Looking specifically at precipitation in northern Brazil, *Uvo et al.* [1998] found that the best correlations were in April and May, corresponding to a delayed response to ENSO-related temperature anomalies in the tropical Atlantic. On the Chilean side of the Andes, the seasonal signal in precipitation peaks in winter, and so a different response may be expected [*Grimm et al.*, 2000].

5. Summary and Conclusions

[27] In this paper we have looked at how three different precipitation data sets portray the large-scale interannual variations associated with the North Atlantic Oscillation and the Southern Oscillation. These two phenomena were both characterized by normalized pressure differences, indicating the change in zonal winds in the appropriate regions. There are marked differences between the data sets in terms of the mean precipitation in certain basins (see Quartly et al., submitted manuscript, 2006), so all analysis here was on anomalies relative to the mean seasonal cycle.

[28] The three data sets showed similar patterns of response to changes in the NAO index (Figures 1a–1c), with the negative NAO phase generally resulting in increased precipitation over Greenland and southwest Europe, with the opposite occurring over the North Atlantic and northwest Europe. The models show the region of negative correlation extending into northwest Africa, but this was not echoed in the GPCP (satellite) data set. *Struglia et al.* [2004] had identified that the flows in several river basins draining into the Mediterranean were significantly anticorrelated with NAO (their Figure 5); our work shows a larger region (Mediterranean Sea plus neighbouring countries) to be significantly affected by NAO. Over the North Atlantic and surrounding land masses, there is no net change in the freshwater input in response to NAO (Figure 2e). However, the different localised freshwater anomalies do not necessarily cancel one another out. The Labrador and Nordic seas are important sites for ocean convection through intense cooling by winds blowing from over the cold land masses. This convection leads to the formation of North Atlantic Deep Water (NADW), but changes in freshwater input will affect the depth of the convection and the salinity of the resultant water mass. Variations in the formation of NADW may affect the so-called Atlantic conveyor belt (thermohaline circulation), altering regional and global climate over a period of many years. Continued study of precipitation over the Labrador and Nordic seas and its response to the NAO is therefore essential if future climate change scenarios are to be fully understood. *Curry et al.* [2003] have linked NAO with significant changes in the freshwater balance of the North Atlantic; our results show that NAO's effects on precipitation are out of phase over the Labrador and Nordic seas. However, in order to make definitive statements about the NAO's impact on the oceanic freshwater budget we would need to take account of evaporation, and that is beyond the scope of this paper.

[29] In a similar manner to the NAO in the North Atlantic, the Southern Oscillation was found to act to redistribute precipitation around the tropical regions of the

world (Figure 3h), with many regions showing a response to changes in the SOI. The most pronounced region is the central and eastern Pacific, where the ITCZ broadens, intensifies and migrates south by several degrees, leading to a much larger flux of freshwater into the ocean at the equator. This is accompanied by eastward movement of the SPCZ, although the models' representation of this feature does not fully match that of the GPCP data set [*Trenberth and Guillemot*, 1998]. The respective time series (Figure 3e) show a clear response to the four El Niño events during the 22-year analysis period. These midocean changes are also accompanied by increased rainfall along the Californian, Mexican and Chilean coasts. This finding is common to all three data sets and corroborated by land-based records [*Castello and Shelton*, 2004; *Pisciottano et al.*, 1994].

[30] The other major region showing a response to El Niño is the area over Indonesia and to its east, where intense atmospheric convection and precipitation occurs in "normal" years. The area has a marked reduction in precipitation during El Niño (leading to drought and increased problems with forest fires). The reduction in rainfall occurs for all four major El Niño events (Figure 3f), but increased precipitation in response to La Niñas is less clearly seen. The region of sensitivity near Indonesia is much smaller in the NCEP data set (Figure 1e) than the other two.

[31] The sensitivity analysis also highlights a region of positive correlation in the tropical Atlantic. This was present in all three data sets, but the attendant time series (Figure 3g) only indicate a clear response for the 1982/1983 and 1997/1998 El Niños, which were the most extreme of the 20th century [*Wolter and Timlin*, 1998]. The net precipitation effect over these three tropical regions — Atlantic, Pacific and Indonesia extending into the Indian Ocean — is that the total rainfall appears to have little sensitivity to the SOI (Figure 3h). (The curve for ECMWF is not shown as its long-term trend requires a much larger scale for display.)

[32] An earlier analysis of the GPCP, NCEP and ECMWF data sets found some major differences in the regional mean precipitation rates and the amplitude and timing of the seasonal variations (Quartly et al., submitted manuscript, 2006). Thus it is somewhat surprising that this study looking at departures from the seasonal cycles showed such consistency between three very different data sets, not only in the location of the regions of positive and negative response, but also in their magnitudes. There are some notable disagreements however and these may suggest deficiencies in particular data sets.

[33] This is one of the first papers (to our knowledge) to look at NAO's effect upon precipitation using data sets spanning both ocean and land. Along the east coast of Greenland the models show a strong negative response to NAO, which is not matched by the satellite data set. This may indicate an exaggerated orographic effect within the models. GPCP shows less response over northeast Europe (Figure 1d) than the others, and also a step change in 1987 in the southern Europe average (Figure 2c). These both indicate a change in the quality of the data set upon inclusion of SSM/I. A closer resemblance is found if only the period 1988–2000 is analysed. A revised version of GPCP removes this discrepancy (see Appendix A).

[34] The SO analysis show no such sensitivity to the inclusion of SSM/I data. A number of explanations come to

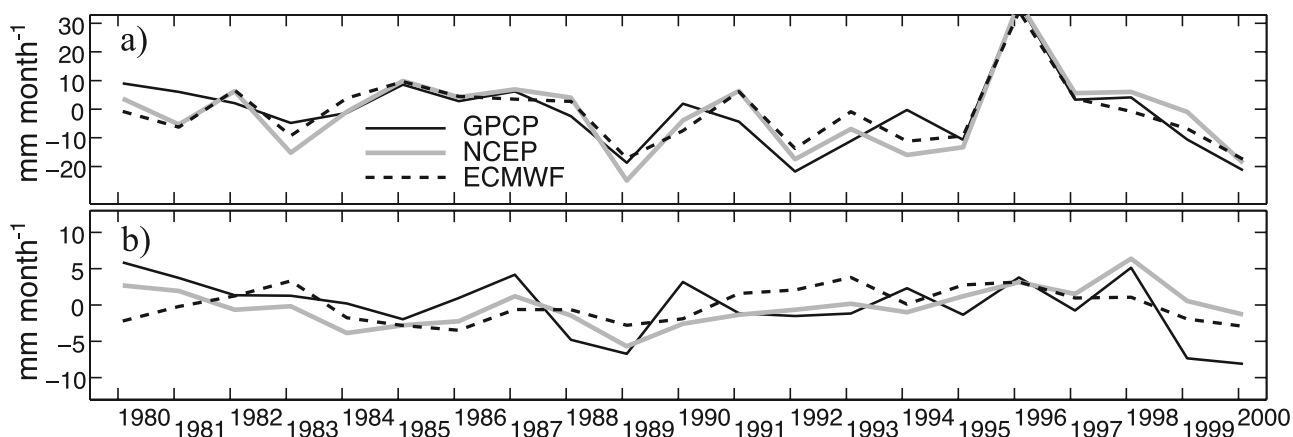


Figure A1. Revised comparison of winter precipitation anomalies using June 2006 version of GPCPv2. (a) southern Europe region; (b) North Atlantic and surrounding land masses (cf. Figures 2c and 2e).

mind. Firstly, the principal SO-affected regions are in the tropics where there is better geostationary coverage by infrared sensors. Secondly, the tropical rainfall is predominantly from large convective cells with attendant cloud tops offering an infrared signature, whereas the North Atlantic storms provide less correlation between the precipitation below the clouds and the signals recorded by pre-1987 sensors. Thirdly, the SO index varies more rapidly than the NAO, and consequently as wide a range of values is found in the 1988–2000 timeframe as before.

[35] Given that precipitation over the tropical oceans in ECMWF is subject to a long-term increase [see *Uppala et al.*, 2004; *Hagemann et al.*, 2005], it is surprising that it is this model whose SO response most closely matches that of GPCP. NCEP is known to exhibit a relatively weak wind field in the tropics [*Josey et al.*, 2002], which explains the weaker precipitation response in the Pacific (Figure 1e). Its precipitation sensitivity over Indonesia is much weaker than in the other two data sets, although land station records suggest that unlike the other two, NCEP has the correct sign of the response over Sumatra.

[36] All three data sets agree on the response over the tropical Atlantic and north Brazil, but NCEP indicates negligible effect in south Brazil, Uruguay and Argentina contrary to the other two data sets and numerous records of land stations [*Ropelewski and Halpert*, 1987; *Grimm et al.*, 2000].

[37] This paper has not attempted to be an exhaustive study of the precipitation response of El Niño, since that would require analysis for separate seasons and/or lagged correlations. Rather, uniquely, here we have applied identical analysis to three different data sets enabling a much better comparison of their responses than can be obtained by comparing separate studies of individual data sets using different El Niño indices [*Hanley et al.*, 2003] and data durations. By combining with an analysis of NAO, we have demonstrated that the problems associated with a particular data set may differ regionally.

[38] We have shown that these three data sets exhibit much in common in their portrayal of interannual changes in precipitation, although we have also highlighted areas of possible problems. It would seem that greater coherence between observations and modelling of present day rainfall

variations is required before models can be fully trusted to predict precipitation patterns under various “greenhouse warming” scenarios.

Appendix A: Latest version of GPCP

[39] A new version of the GPCP v2 multisatellite data set became available in late June 2006, after this paper was accepted. This amended the rain rate over land in the SSM/I era (post 1987) to achieve a closer match to gauge data (D. Bolvin, personal communication, 2006). This revision to the data set showed increased rain rates over the whole European continent, but no change for ocean pixels. Upon repeating our analysis, the northern Europe and southern Europe regions that showed significant sensitivity to NAO became slightly larger than portrayed in Figure 1a, but the time series of mean anomalies over Greenland and northern Europe were essentially unchanged. However, with the new data set, there is no longer a step change in precipitation anomaly at 1988 for either southern Europe (Figure A1a) or over the extended North Atlantic region (Figure A1b).

[40] The revision to the data set made negligible change to the ENSO analysis.

[41] **Acknowledgments.** We are grateful to GPCP, NCEP, and ECMWF for the free provision of their data, to Simon Josey for retrieval and early processing of the data, and to George Huffman and Per Kållberg for clarification of information concerning the products.

References

- Adler, R. F., C. Kidd, G. Petty, M. Morissey, and H. M. Goodman (2001), Intercomparison of global precipitation products: The third precipitation intercomparison project (PIP-3), *Bull. Am. Meteorol. Soc.*, **82**, 1377–1396.
- Adler, R. F., et al. (2003), The version-2 Global Precipitation Climatology Project (GPCP) monthly precipitation analysis (1979–present), *J. Hydro-meteorol.*, **4**, 1147–1167.
- Andrews, E. D., R. C. Antweiler, P. J. Neiman, and F. M. Ralph (2004), Influence of ENSO on flood frequency along the California coast, *Int. J. Climatol.*, **17**, 337–348.
- Barlow, M., H. Cullen, and B. Lyon (2002), Drought in central and south-west Asia: La Niña, the warm pool, and Indian Ocean precipitation, *Int. J. Climatol.*, **15**, 697–700.
- Barrett, E. C., and D. W. Martin (1981), *The Use of Satellite Data in Rainfall Monitoring*, Elsevier, New York.
- Bojariu, R., and G. Reverdin (2002), Large-scale variability modes of freshwater flux and precipitation over the Atlantic, *Clim. Dyn.*, **18**, 369–381, doi:10.1007/s003820100182.

- Bromwich, D. H., Q. Chen, Y. Li, and R. T. Cullather (1999), Precipitation over Greenland and its relation to the North Atlantic Oscillation, *J. Geophys. Res.*, *104*, 22,103–22,115.
- Castello, A. F., and M. L. Shelton (2004), Winter precipitation on the US Pacific coast and El Niño-Southern Oscillation events, *Int. J. Climatol.*, *24*, 481–497.
- Chang, C.-P., Z. Wang, J. Ju, and T. Li (2004), On the relationship between western maritime continent monsoon rainfall and ENSO during northern winter, *J. Clim.*, *17*, 665–672.
- Curry, R., B. Dickson, and I. Yashayaev (2003), A change in the freshwater balance of the Atlantic Ocean over the past four decades, *Nature*, *426*, 826–829.
- Dai, A., and T. M. L. Wigley (2000), Global patterns of ENSO-induced precipitation, *Geophys. Res. Lett.*, *27*, 1283–1286.
- Dorman, C. E., and R. H. Bourke (1981), Precipitation over the Atlantic Ocean, 30°S to 70°N, *Mon. Weather Rev.*, *109*, 554–563.
- Geophysical Fluid Dynamics Laboratory Global Atmospheric Model Development Team (GFDL) (2004), The new GFDL global atmosphere and land model AM2-LM2: Evaluation with prescribed SST simulations, *J. Clim.*, *17*, 4641–4663.
- Georgakakos, K. P. (1998), Flooding attributable to El Niño, *WMO Bull.*, *47*, 356–360.
- Goodess, C. M., and P. D. Jones (2002), Links between circulation and changes in the characteristics of Iberian rainfall, *Int. J. Climatol.*, *22*, 1593–1615.
- Grimm, A. M. (2003), The El Niño impact on the summer monsoon in Brazil: Regional processes versus remote influences, *J. Clim.*, *16*, 263–280.
- Grimm, A. M., V. R. Barros, and M. E. Doyle (2000), Climate variability in southern South America associated with El Niño and La Niña events, *J. Clim.*, *13*, 35–58.
- Gruber, A., X. Su, M. Kanamitsu, and J. Schemm (2000), The comparison of two merged rain gauge-satellite precipitation data sets, *Bull. Am. Meteorol. Soc.*, *81*, 2631–2644.
- Hagemann, S., K. Arpe, and L. Bengtsson (2005), Validation of the hydrological cycle of ERA-40, *ERA-40 Proj. Rep. Ser. 24*, Eur. Cent. for Medium-Range Weather Forecasts, Reading, U. K.
- Hanley, D. E., M. A. Bourassa, J. J. O'Brien, S. R. Smith, and E. R. Spade (2003), A quantitative evaluation of ENSO indices, *J. Clim.*, *16*, 1249–1258.
- Hastenrath, S. (1978), On modes of tropical circulation and climate anomalies, *J. Atmos. Sci.*, *35*, 2222–2231.
- Huffman, G. J., et al. (1997), The global precipitation climatology project (GPCP) combined precipitation data set, *Bull. Am. Meteorol. Soc.*, *78*, 5–20.
- Hurrell, J. W. (1995), Decadal trends in the North Atlantic Oscillation: Regional temperatures and precipitation, *Science*, *269*, 676–679.
- Josey, S. A., and R. Marsh (2005), Surface freshwater flux variability and recent freshening of the North Atlantic in the eastern subpolar gyre, *J. Geophys. Res.*, *110*, C05008, doi:10.1029/2004JC002521.
- Josey, S. A., E. C. Kent, and P. K. Taylor (2002), Wind stress forcing of the ocean in the SOC climatology: Comparisons with the NCEP-NCAR, ECMWF, UWM/COADS, and Hellerman and Rosenstein data sets, *J. Phys. Oceanogr.*, *32*, 1993–2019.
- Khalil, M. A. K., W. Zhao, and R. M. Mackay (1992), Climatic change: Relationship between temperature and precipitation, in *Encyclopedia of Earth System Science*, vol. 1, edited by W. A. Nierenberg, pp. 525–533, Elsevier, New York.
- Kistler, R., et al. (2001), The NCEP-NCAR 50-year reanalysis: Monthly means CD-ROM and documentation, *Bull. Am. Meteorol. Soc.*, *82*, 247–267.
- Mass, C. F., and D. A. Portman (1989), Major volcanic eruptions and climate: A critical evaluation, *J. Clim.*, *2*, 566–593.
- Nicholson, S. E. (1997), An analysis of the ENSO signal in the tropical Atlantic and western Indian Oceans, *Int. J. Climatol.*, *17*, 345–375.
- Nicholson, S. E., D. Leposo, and J. Grist (2001), The relationship between El Niño and drought over Botswana, *J. Clim.*, *14*, 323–335.
- Ntale, H. K., and T. Y. Gan (2004), East African rainfall anomaly patterns in association with El Niño/Southern Oscillation, *J. Hydrol. Eng.*, *9*, 257–268.
- Ogi, M., Y. Tachibana, and K. Yamazaki (2003), Impact of the wintertime North Atlantic Oscillation (NAO) on the summertime atmospheric circulation, *Geophys. Res. Lett.*, *30*(13), 1704, doi:10.1029/2003GL017280.
- Pettersen, S. (1969), *Introduction to Meteorology*, 3rd ed., McGraw-Hill, New York.
- Pisciottano, G., A. Diaz, G. Cazes, and C. R. Mechoso (1994), El Niño-Southern Oscillation impact on rainfall in Uruguay, *J. Clim.*, *7*, 1286–1302.
- Quartly, G. D., M. A. Srokosz, and T. H. Guymer (2000), Changes in oceanic precipitation during the 1997–98 El Niño, *Geophys. Res. Lett.*, *27*, 2293–2296.
- Quartly, G. D., T. H. Guymer, and K. G. Birch (2002), Back to basics: Measuring rainfall at sea: Part 1—In situ sensors, *Weather*, *57*, 315–320.
- Ropelewski, C. F., and M. S. Halpert (1987), Global and regional scale precipitation patterns associated with the El Niño/Southern Oscillation, *Mon. Weather Rev.*, *115*, 1606–1626.
- Sohn, B. J., E. A. Smith, F. R. Robertson, and S. C. Park (2004), Derived over-ocean water vapor transports from satellite-retrieved E-P data sets, *J. Clim.*, *17*, 1352–1365.
- Struglia, M. V., A. Mariotti, and A. Filogrosso (2004), River discharge into the Mediterranean Sea: Climatology and aspects of the observed variability, *J. Clim.*, *17*, 4740–4751.
- Taylor, P. K. (2000), Intercomparison and validation of ocean-atmosphere energy flux fields, *Rep. WCRP-112*, World Clim. Res. Programme, Geneva, Switzerland.
- Trenberth, K. E. (1984), Signal versus noise in the Southern Oscillation, *Mon. Weather Rev.*, *112*, 326–332.
- Trenberth, K. E., and C. J. Guillemot (1998), Evaluation of the atmospheric moisture and hydrological cycle in the NCEP/NCAR reanalyses, *Clim. Dyn.*, *14*, 213–231.
- Troccoli, A., and P. Källberg (2004), Precipitation correction in the ERA-40 reanalysis, *ERA-40 Proj. Rep. Ser. 13*, Eur. Cent. for Medium-Range Weather Forecasts, Reading, U. K.
- Tsimplis, M. N., and S. A. Josey (2001), Forcing of the Mediterranean Sea by atmospheric oscillations over the North Atlantic, *Geophys. Res. Lett.*, *28*, 803–806.
- Tucker, G. G. (1961), Precipitation over the North Atlantic Ocean, *Q. J. R. Meteorol. Soc.*, *87*, 147–158.
- Uppala, S., P. Källberg, A. Hernández, S. Saarinen, M. Fiorino, X. Li, K. Onogi, N. Sokka, U. Andrae, and V. Da Costa Bechtold (2004), ERA-40: ECMWF 45-year reanalysis of the global atmosphere and surface conditions 1957–2002, *News1. 101*, pp. 2–21, Eur. Cent. for Medium-Range Weather Forecasts, Reading, U. K.
- Uvo, C. B., C. A. Repelli, S. E. Zebiak, and Y. Kushnir (1998), The relationships between tropical Pacific and Atlantic SST and northeast Brazil monthly precipitation, *J. Clim.*, *11*, 551–562.
- Wolter, K., and M. S. Timlin (1998), Measuring the strength of ENSO events: How does 1997/98 rank?, *Weather*, *53*, 315–324.
- Woodworth, P. L., and D. L. Blackman (2004), Evidence for systematic changes in extreme high waters since the mid-1970s, *J. Clim.*, *17*, 1190–1197.
- Xie, P., and P. Arkin (1997), Global precipitation: A 17-year monthly analysis based on gauge observations, satellite estimates, and numerical model outputs, *Bull. Am. Meteorol. Soc.*, *78*, 2539–2558.

E. A. Kyte, School of Ocean Sciences, University of Wales Bangor, Menai Bridge, Anglesey, LL59 5AB, UK.

G. D. Quartly, M. A. Srokosz, and M. N. Tsimplis, National Oceanography Centre, Empress Dock, Southampton, SO14 3ZH, U.K. (gdq@noc.soton.ac.uk)